IMEKO International Conference on
Metrology for Archaeology and Cultural Heritage
Lecce, Italy, October 23-25, 2017

# Health Monitoring of a Matured Tree Using Ground Penetrating Radar – Investigation of the Tree Root System and Soil Interaction

Amir. M. Alani[1], Luca Bianchini Ciampoli[2], Fabio Tosti[1], Maria Giulia Brancadoro[1], Daniele Pirrone[2], Andrea Benedetto[2]

[1] *School of Computing and Engineering, University of West London (UWL), St Mary's Road, Ealing, W5 5RF, London, UK, Amir.Alani@uwl.ac.uk; Fabio.Tosti@uwl.ac.uk; 21358807@student.uwl.ac.uk*

[2] *Department of Engineering, Roma Tre University, Via Vito Volterra 62, 00146 Rome, Italy, luca.bianchiniciampoli@uniroma3.it; daniele.pirrone20@gmail.com; andrea.benedetto@uniroma3.it*

***Abstract* – In this study, a demonstration of the ground penetrating radar (GPR) potential in the health monitoring of a matured tree has been given. The main objectives of the research were to provide an effective mapping of the tree roots as well as reliable simulation scenarios representing a variety of possible internal defects in terms of shape and formation. To these purposes, the soil around a 70-year-old fir tree, with a trunk circumference of 3.40 m and an average radius of 0.55 m, was investigated. A ground-coupled multi-frequency GPR system equipped with 600 MHz and 1600 MHz central frequency antennas was used for testing purposes. In addition to the above objective, finite-difference time-domain (FDTD) simulations of the electromagnetic field propagation through the cross-section of a trunk (consistent with the investigated fir tree) were carried out. A variety of defects representing cavities created due to decay were also simulated. The results from the simulations proved significant potential for the interpretation of complex decay phenomena within the trunk.**

## I. INTRODUCTION

The sensibility towards environmental issues along with the attention on preserving natural heritage, especially ancient trees and rare plants, has greatly increased, and the management and control of the forestall heritage and the floral system has become accordingly a high-priority objective to achieve. One of the main factors of tree decay which originally gained public attention is the presence of unknown pathogens carried along by the wind, which can lead to epidemic phenomena and often to a quick death of entire forests [1]. In such an emergency situation, two main approaches can be followed, namely, i) active measures, i.e., the avoidance of any contact between the pathogenic spores and the trees using bio-security measures at the boundaries of the interested region/country, and ii) passive measures, i.e., the application of policies for the control and the management of the forestall heritage aimed at identifying the early-stage symptoms of disease and the eradication or the limitation of their impacts [2]. Since the latest approach is based on the monitoring of living trees, invasive methods of health assessment such as cutting off branches or incremental coring are increasingly discouraged, and a non-destructive assessment proves to be the only option to undertake. Among the available non-destructive testing (NDT) methods, ground-penetrating radar (GPR) is gaining momentum due to the high versatility, rapidity of data collection and the provision of reliable results at relatively limited costs [3, 4].

GPR is a geophysical non-destructive method that can be traced back to the nineteen fifties [5] and, historically, its first major use was in demining operations [6]. Due to the large availability of antenna configurations and the technological developments of the hardware and software components, it is now used in a wide range of disciplines, spanning planetary explorations [7], civil and environmental engineering [8, 9], geology [10], archaeology [11], forensic and public safety [12], agricultural and forestry sciences [13, 14].

The first application of GPR in tree health monitoring can be traced back to 1999 and relates to the mapping of tree root systems [15]. From that time onward, several GPR applications followed and were focused on the analysis of the complexities of trunk and root systems. With regard to the investigation of tree root systems, the research was mostly focused on the assessment of the root diameter [16], biomass [17], coarseness [18] and pattern in complex urban areas [19]. For the investigation of the tree trunks, factors like the inner structure [20, 21],

the anisotropy (grain orientation) [22, 23], water content [24] and the frequency of the applied electromagnetic (EM) field [25] were mostly analysed. Research was focused on survey techniques such as the use of planar [26] or arc [27] perfect electric conductors (PEC). On the contrary, the use of the numerical simulation of the GPR signal for the interpretation of the geometric and physical characteristics and decay processes of trunks [27] is much more recent.

## II. AIMS AND OBJECTIVES

The aim of this research was to demonstrate and investigate the effectiveness of the GPR in the health monitoring and assessment of trees and tree roots and soil interaction. The main objectives of the research were:

- to provide an effective method of mapping tree roots as well as to establish reliable simulation scenarios representing possible internal defects in the tree trunk (in terms of shape and formation);
- to create a set of finite-difference time-domain (FDTD) simulations of the electromagnetic (EM) field propagation through the cross-section of a tree trunk.

## III. METHODOLOGY

### *A. Investigation of the tree root system*

#### *1) The Survey Technique*

The soil around a 70-year-old fir tree, with a trunk circumference of 3.40 m and an average radius of 0.55 m, was investigated. 9 circular scans, 0.30 m from one another, were carried out all around the tree circumference from 0.50 m the outer surface of the bark. A ground-coupled multi-frequency GPR system equipped with 600 MHz and 1600 MHz central frequency antennas was used for testing purposes. Data were acquired using a time window of 40 ns and 512 samples. The horizontal resolution was set to $2.4 \times 10^{-2}$ m. In order to reach the maximum penetration depth of the root system, only the 600 MHz frequency was considered for data processing purposes. A swept circle area with an outer radius of 3.45 m and an inner radius of 1.05 m was finally scanned.

#### *2) The Signal Processing Scheme*

Four main steps were carried out to identify the tree root system under the investigated area. First, signal noise filtering was applied by the sequential use of time-zero correction, zero-offset removal and bandpass filtering. Second, background removal was applied to filter out the reflections from the flat layers. One of the main effects of this filter was to remove the reflection from the ground. In the third step, the GPR scans were converted from the Cartesian to the polar coordinate system. Hence, a three-dimensional (3-D) cylindrical domain with origin at the intersection between the vertical axis of the tree trunk and the ground plane was built.


*Fig. 1. Circular scans performed around the investigated 70-years old fir tree.*

Finally, an amplitude threshold was set according to literature values for similar trees in highly-wet conditions [24], which were related to the presence of roots. This allowed to filter out from the 3-D matrix the amplitude values not likely related to the tree roots.

### *B. Numerical Simulations*

A tree trunk section with geometric characteristics similar to the actual fir tree was reproduced using numerical modelling. To this effect, the numerical simulator package gprMax 2D was used [28]. The design of the gprMax models and their distributed execution on multicore machines was aided by the freeware tool E2GPR [29].

The cross-section of the trunk was represented by non-concentric rings. One transmitter *tx* and one receiver *rx* were initially positioned at $\theta = 0°$, as it is indicated in Fig. 2a. The FDTD simulations were run counter-clockwise from $\theta = 0°$ to $\theta = 360°$ along the circumference inscribing the tree trunk cross-section. The side of the square inscribing the mentioned circumference was 1 m, such that the radius of the simulated trunk was approximately 0.5 m. With regard to the reference (undamaged) trunk cross-section (i.e., Scenario 0), permittivity values that increased from the bark ($\varepsilon_r = 4$) to the heartwood ($\varepsilon_r = 22$) were assumed (see the legend in Fig. 2a). This was done to make the dielectric boundary conditions of the materials more representative of the physical conditions of the tree trunk in a humid environment at the peak of the daylight (i.e., actual testing conditions). Furthermore, a variety of defects representing rotting and cavities created due to decay was simulated. Three different scenarios were considered in this study: i) concentric damage representing the action of rotting in one of the inner rings (i.e., Scenario I, Fig. 2b); ii) air cavity at the boundary area between heartwood/most internal ring (i.e., Scenario II, Fig. 2c); iii) rotten cavity at the boundary area between heartwood/most internal ring (i.e., Scenario III, Fig. 2d).

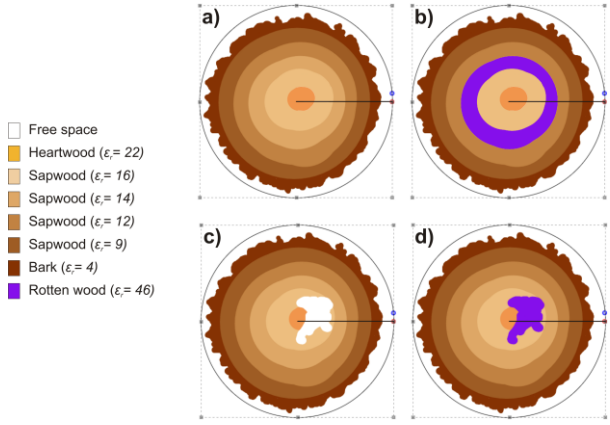


*Fig. 2. Modelled cross-section of the tree trunk: undamaged case (Scenario 0) (a); with a concentric (rotten) damage (Scen. I) (b); with an air cavity at the boundary area between heartwood/most internal ring (Scen. II) (c); with a rotten cavity at the boundary area between heartwood/most internal ring (Scen. III) (d).*

## IV. RESULTS AND SHORT DISCUSSION

### *A. Investigation of the tree root system*

From the 3-D cylindrical domain obtained by the aforementioned processing scheme, several visualisation modes were extracted. Figure 3 shows one B-scan extrapolated radially at one generic position within the investigated swept circle area. In addition, the use of tomographic amplitude maps (e.g., Fig. 4) allowed for a more comprehensive interpretation of the data from shallow depths up to a maximum depth $z$ = 1.56 m.

The processing scheme mentioned in Section III was followed for the visualisation of the tree root system. The red spots in the 3-D view depicted in Fig. 5 represent the pattern of the tree roots as per the threshold defined above. For the sake of consistency, the coordinates of these points were double-checked with the positions of the hyperbola apexes identified in the collected B-scans.

### *B. Numerical Simulations*

The results from the simulations demonstrated significant potential for the interpretation of complex decay phenomena within a tree trunk.

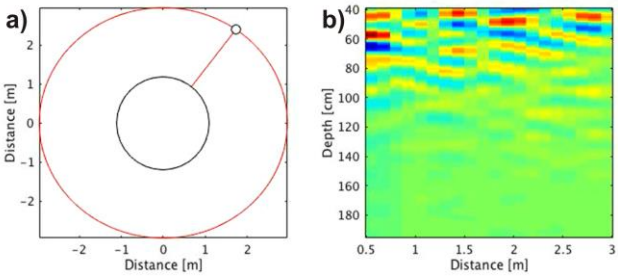


*Fig. 3. Radial B-scan processing: scan within the swept circle area (a) and relevant extrapolated B-scan (b).*

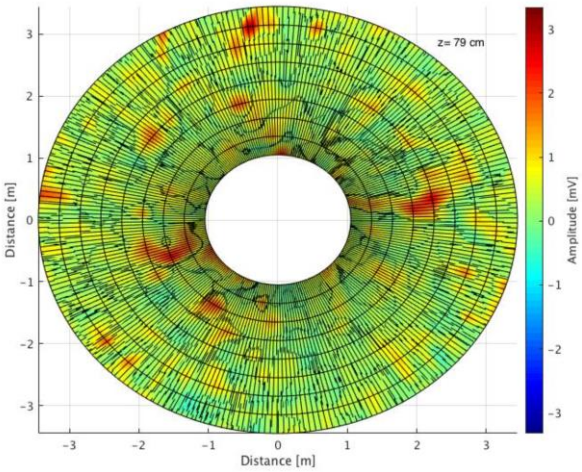


*Fig. 4. Tomographic amplitude map extrapolated from the 3-D cylindrical domain at depth z = 79 cm.*

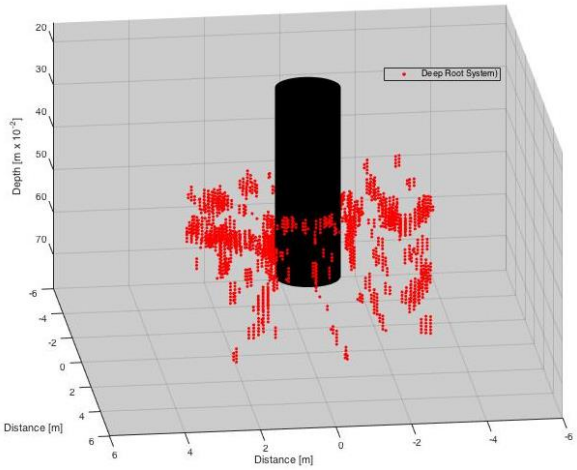


*Fig. 5. Three-dimensional view of the tree root system after the application of the dedicated signal processing scheme.*

With regard to the reference (undamaged) cross-section (Fig. 6a), the reflected waves from the interfaces between the rings are clearly visible.

On the contrary, in the case of the rotten ring (i.e., the concentric damage) (Fig. 6b), the waves are reflected from the higher permittivity contrast, which hides the reflections from the inner rings.

In the case of Scenario II (i.e., the cross-section with an air cavity at the boundary area between the heartwood and the most internal ring) (Fig. 6c), it is clearly visible a wave reflected at the air cavity area.

The reflections coming from the forward ring interfaces are still visible. A similar bouncing at the damage interface with no further distinctions of the forward reflections from the rings is instead shown at Scenario III (i.e., cross-section with a rotten cavity at the boundary area between the heartwood and the most internal ring) (Fig. 6d).

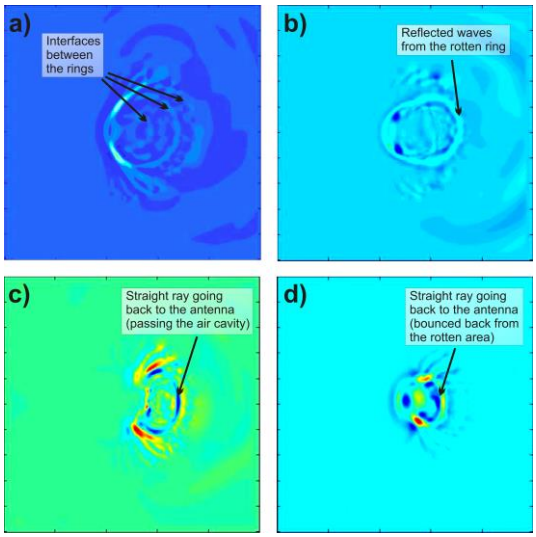


*Fig. 6. Snapshots of the electric field intensity: Scenario 0 (a); Scenario I (b); Scenario II (c); Scenario III (d).*

## V. CONCLUSION

This paper reports a demonstration of the ground penetrating radar (GPR) potential in the health monitoring of a matured tree. The main objectives of the research were to provide an effective mapping of the tree roots as well as reliable simulation scenarios representing a variety of possible internal defects in terms of shape and formation. In view of the above, the soil around a 70-years old fir tree, with a trunk circumference of 3.40 m and an average radius of 0.55 m, was investigated. A ground-coupled multi-frequency GPR system equipped with 600 MHz and 1600 MHz central frequency antennas was used for testing purposes. The here proposed signal processing scheme allowed to track the tree root system with the 600 MHz antenna frequency after cross-checking the identified path with the position of the hyperbola apexes within the collected B-scans.

In addition to the above objective, finite-difference time-domain (FDTD) simulations of the electromagnetic field propagation through the cross-section of a trunk were carried out. To this purpose, the numerical simulator package gprMax 2D was used. The freeware tool E2GPR aided the design of the gprMax models and their distributed execution on multicore machines. Furthermore, a variety of defects representing cavities created due to decay was simulated. The results from the simulations demonstrated significant potential for the interpretation of complex decay phenomena within the trunk. In more detail, the presence of rotten areas and air cavities with high permittivity contrast between the surrounding materials was clearly detected. Furthermore, the ability to hide further (expected) reflections from the next interfaces was a distinctive feature of the presence of rotting within the trunk cross-section.

## ACKNOWLEDGMENT

The authors are sincerely grateful to Mr Spartaco Cera for the invaluable help during the GPR surveys.

## REFERENCES

[1] Robinson R. A., 2012. Plant Pathosystems. Springer Science and Business Media. 186 pp.

[2] Alverson W. S., Kuhlmann W., and Waller D., 1994. Wild forests: conservation biology and public forests. 300 pp.

[3] Lorenzo H., Pérez-Gracia V., Novo A., and Armesto J., 2010. Forestry applications of ground-penetrating radar [Aplicaciones forestales del radar de subsuelo]. Forest Systems, 19 (1): 5-17.

[4] Bassuk N., Grabosky J., Mucciardi A., and Raffel G., 2011. Ground-penetrating radar accurately locates tree roots in two soil media under pavement. Arboriculture and Urban Forestry, 37 (4): 160-166.

[5] El Said M, 1956. Geophysical prospection of underground water in the desert by means of electromagnetic interference fringes, in Proc. I.R.E., 44: 24–30.

[6] Potin D., Duflos E., and Vanheeghe P., 2006. Landmines ground-penetrating radar signal enhancement by digital filtering, IEEE Transactions on Geoscience and Remote Sensing, 44 (9): 2393-2406.

[7] Tosti F. and Pajewski L., 2015. Applications of radar systems in Planetary Sciences: an overview Chapt. 15 - Civil Engineering Applications of Ground Penetrating Radar, Springer Transactions in Civil and Environmental Engineering Book Series, pp. 361–371.

[8] Benedetto A. and Pajewski L., 2015. Civil Engineering Applications of Ground Penetrating Radar. Springer Transactions in Civil and Environmental Engineering Book Series.

[9] Alani, A. M., Aboutalebi, M., and Kilic, G., 2013. Applications of ground penetrating radar (GPR) in bridge deck monitoring and assessment. Journal of Applied Geophysics, 97: 45-54.

[10] Benson A. K., 2001. Applications of ground penetrating radar in assessing some geological hazards: examples of groundwater contamination, faults, cavities," Journal of Applied Geophysics, 33 (1-3): 177–193.

[11] Goodman D., 1994. Ground-penetrating radar simulation in engineering and archaeology, Geophysics, 59 (2): 224-232, 1994.

[12] Schultz J. J., Collins M. E., and Falsetti A. B., 2006. Sequential monitoring of burials containing large pig cadavers using ground-penetrating radar," Journal of Forensic Sciences, 3: 607-616.

[13] Lambot S., Weihermüller L., Huisman J. A., Vereecken H., Vanclooster M. and Slob E. C., 2006. Analysis of air-launched ground-penetrating radar

techniques to measure the soil surface water content. Water Resources Research 42(11): W11403. doi: 10.1029/2006WR005097.

[14] Butnor J.R., Doolittle J.A., Kress L., Cohen S., and Johnsen K.H., 2001. Use of ground-penetrating radar to study tree roots in the southeastern United States. Tree Physiology, 21 (17): 1269-1278.

[15] Hruska, J., Cermák, J., Sustek, S. Mapping tree root systems with ground-penetrating radar (1999) Tree Physiology, 19 (2): 125-130.

[16] Barton, C.V.M., Montagu, K.D. Detection of tree roots and determination of root diameters by ground penetrating radar under optimal conditions (2004) Tree Physiology, 24 (12): 1323-1331.

[17] Butnor, J.R., Doolittle, J.A., Johnsen, K.H., Samuelson, L., Stokes, T., Kress, L. Utility of ground-penetrating radar as a root biomass survey tool in forest systems (2003) Soil Science Society of America Journal, 67 (5): 1607-1615.

[18] Guo, L., Chen, J., Cui, X., Fan, B., Lin, H. Application of ground penetrating radar for coarse root detection and quantification: A review (2013) Plant and Soil, 362 (1-2), pp. 1-23.

[19] Stokes, A., Fourcaud, T., Hruska, J., Cermak, J., Nadyezdhina, N., Nadyezhdin, V., Praus, L. An evaluation of different methods to investigate root system architecture of urban trees in situ: I. ground-penetrating radar (2002) Journal of Arboriculture, 28 (1): 2-10.

[20] Nicolotti G., Socco L.V., Martinis R., Godio A., Sambuelli L., 2003. Application and comparison of three tomographic techniques for detection decay in trees, J. Arboric., 29 (2): 66–78.

[21] Butnor J.R., Pruyn M.L., Shaw D.C., Harmon M.E., Mucciardi A.N., and Ryan M.G., 2009. Detecting defects in conifers with ground penetrating radar: applications and challenges, Forest Pathol., 39 (5): 309–322.

[22] Rodríguez-Abad I., Martínez-Sala R., García-García F., and Capuz-Lladro R., 2010. Nondestructive methodologies for the evaluation of moisture content in sawn timber structures: ground-penetrating radar and ultrasound techniques, Near Surf. Geophys. 8: 475–482.

[23] Martínez-Sala R., Rodríguez-Abad I., Diez Barra R., and Capuz-Lladró R., 2013. Assessment of the dielectric anisotropy in timber using the nondestructive GPR technique, Constr. Build. Mater., 38: 903–911.

[24] Rodríguez-Abad I., Martínez-Sala R., Capuz Lladró R., Díez Barra R., and GarcíaGarcía F., 2011. Assessment of the variation of the moisture content in the pinus pinaster Ait using the non destructive GPR technique, Mater. Constr., 61 (301): 143–156.

[25] Sahin H., and Ay N., 2004. Dielectric properties of hardwood species at microwave frequencies, J. Wood Sci., 50 (4): 375–380.

[26] Lorenzo H., Pérez-Gracia V., Novo A., and Armesto J., 2010. Forestry applications of ground-penetrating radar, Forest Syst., 19 (1): 5–17.

[27] Ježová J., Mertens L., and Lambot S., 2016. Ground-penetrating radar for observing tree trunks and other cylindrical objects, Construction and Building Materials, 123: 214-225.

[28] Giannopoulos A., 2005. Modelling Ground Penetrating Radar by gprMax, Construction and Building Materials, 19: 755–762.

[29] Pirrone D., and Pajewski L. 2015. E2GPR – Edit your geometry, Execute GprMax2D and Plot the Results!, Proc. 2015 IEEE 15th Mediterranean Microwave Symposium, 30 November-2 December 2015, Lecce, Italy, pp. 1-4.